

Lithographically Generated 2D Bi₂Se₃ Grid Patterns as Physical Reservoir Computing Network Devices

Xiaoqiu An, Guanyu Lu, and Xiaogan Liang

Mechanical Engineering Department, University of Michigan, Ann Arbor, MI 48109

anxiaoqi@umich.edu

In our EIPBN 2025 presentation, we presented the nanofabrication of micro/nanoscale Bi₂Se₃ grid structures with memristive channels. These network-like structures can function as physical reservoir layers for hardware-based reservoir computing (RC) devices.¹ While this work highlighted the potential of such Bi₂Se₃ memristive RC devices for practical neuromorphic computing applications, the fundamental device physics mechanisms by which Bi₂Se₃ memristive networks operate as effective neuromorphic reservoirs has not been well understood yet. In particular, it remains unclear how network structure governs device-level dynamics.

In this work, we conduct a systematic principle study on Bi₂Se₃ memristive networks as physical RC devices. In particular, by increasing the grid complexity of cross-linked memristive network patterns, we reveal a direct connection between spatial density, channel interconnectivity, and the nonlinear dynamic diversity intrinsic to reservoir computation.

Fig. 1 presents optical microscopy (OM) images of as-fabricated Bi₂Se₃ memristive network patterns with different grid densities (i.e., 3×3 , 6×6 , and 9×9) within the same device footprint area of 1 mm², which are fabricated using rubbing-induced site-selective deposition (RISS) method.² Such a set of grid network devices exhibit progressively more complex and more interconnected channel morphologies. To ensure that each device reliably functions as a reservoir, we evaluate each network device using Mackey–Glass time-series dynamic prediction (Fig. 2).³ Successful prediction performance across all devices confirms the presence of sufficient nonlinearity and short-term memory for enabling the reservoir computing function.

Building on the aforementioned validation, we further investigate the impact of network architecture on reservoir dynamics by quantitatively comparing the dynamic responses of individual output channels under multiple input waveforms. Reservoir performance is evaluated using normalized root-mean-square error (NRMSE) and coefficient of determination (R²) between input and channel responses (Figs. 3 and 4). Our results show that as the grid density increases from 3×3 to 6×6 , the NRMSE increases significantly while R² decreases, indicating enhanced nonlinear response and stronger short-term memory effects. In contrast, further increasing the density from 6×6 to 9×9 results in minimal changes in both metrics, with only two channels exhibiting huge changes, suggesting saturation of the reservoir dynamics. This trend is consistent with the morphological evolution observed in Fig. 1.

This work establishes a mechanistic understanding of how 2D Bi₂Se₃ network patterns can function as effective physical reservoir computing devices, demonstrating that grid network density governs nonlinear response, short-term memory, and computational complexity. These insights provide a solid foundation for the rational design and fabrication of memristive RC hardware for neuromorphic computing and control applications.

¹ Mingze Chen et al., Nanoelectronics-enabled reservoir computing hardware for real-time robotic controls. *Sci. Adv.* 11, eadu2663 (2025).

² Mingze Chen, Xiaoqiu An, Seungjun Ki, Xiaogan Liang; Rubbing-induced site-selective deposition of 2D material patterns on nanomembranes. *J. Vac. Sci. Technol. B* 1 November 2024; 42 (6): 062801.

³ J. Moon, W. Ma, J. H. Shin, F. Cai, C. Du, S. H. Lee, and W. D. Lu, “Temporal data classification and forecasting using a memristor-based reservoir computing system,” *Nature Electronics*, vol. 2, no. 10, pp. 480–487, 2019.

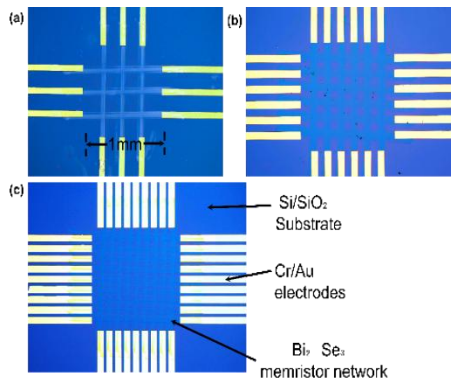


Figure 1: Optical microscopy (OM) images of 2D Bi_2Se_3 grid networks fabricated within a 1 mm^2 footprint area, displaying increasing grid density from 3×3 to 6×6 and 9×9 .

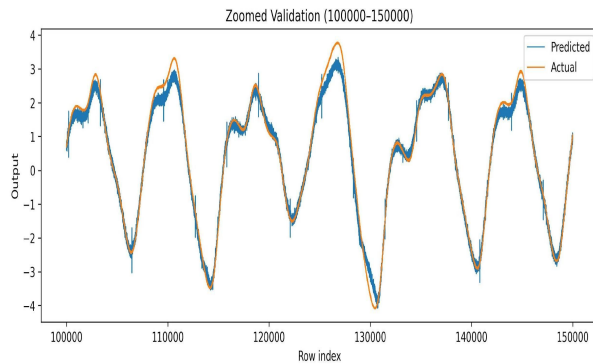


Figure 2: Mackey–Glass time-series dynamic prediction results obtained from a representative Bi_2Se_3 memristive network.

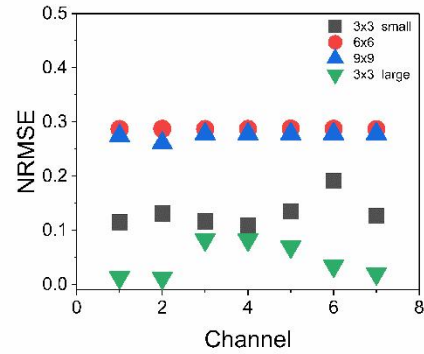


Figure 3: Normalized root-mean-square error (NRMSE) of the voltage response signals captured at seven output channels of four Bi_2Se_3 memristive networks with different grid densities.

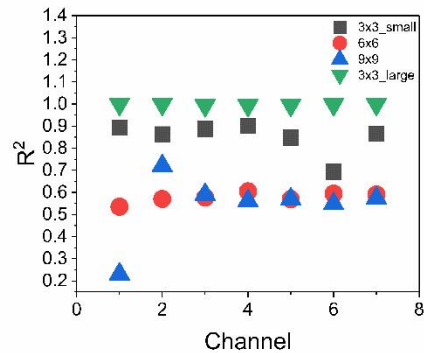


Figure 4: Coefficient of determination (R^2) of the voltage response signals captured at seven output channels of four Bi_2Se_3 memristive networks with different grid densities.